This is not a peer-reviewed article.
Pp. 137-147 in Automation Technology for Off-Road Equipment, Proceedings of the July 26-27, 2002 Conference (Chicago, Illinois, USA) Publication Date July 26, 2002.
ASAE Publication Number 701P0502, ed. Qin Zhang.

Modeling of a Pushed/Pulled Driven Wheel

A. Osetinsky [1] and I. Shmulevich[2]

ABSTRACT

A comprehensive method for off-road pushed/pulled driven wheel modeling is presented, assuming that the soil-wheel contact surface is parabolic. A soil-wheel interaction model was developed, considering steady state and kinematic conditions. The method was verified by experimental data reported in the literature. Traction performance of a driven wheel can be predicted both for driving and braking modes. The model shows significant non-symmetry of the traction wheel performance for driving and braking modes. The braking force developed in braking mode is significantly greater than the traction force reached in driving mode. This method can serve as a comprehensive tool for predicting off-road vehicle performance.

KEYWORDS. Net traction, Gross traction, Off-road, Soil sinkage, Deformation, Slip, Moment.

INTRODUCTION

Traction performance of 4WD vehicles is affected by an internal interaction between driven axles. This results in different values of wheel slip and traction force for each axle. In order to optimize the traction performance of the vehicle, the well-known models reported in literature for predicting wheel traction performance should also be extended for braking mode.

Numerous researchers reported predictions of off-road tire performances, along the years. Some dealt in analytical approaches, others in semi-empirical or empirical approaches. The diversity in approaches of research on off-road tire performance points to the complexity of the issue. Each of the above-mentioned approaches has some limitations: the analytical approaches are difficult to use; empirical equations are limited to the tested cases and most semi-empirical methods focus on predicting separate performances in braking and driving modes. The motivation of this paper is to develop a semi-empirical model for a driven wheel in braking and driving modes, which will combine the measured soil and wheel properties.

Evaluation of traction performance for a driving wheel needs to consider the soil-wheel interaction in two interrelated aspects – steady state motion and kinematics. In order to model the wheel-soil interaction, the form of the contact surface should be determined. The exact solution of this problem is complex. A simple analytical presentation of the contact surface is required.

This work focused on developing a semi-empirical model for prediction of traction performance of a driven wheel, verified by experimental data, and presents a prediction method for off-road wheel performance.

SOIL SINKAGE UNDER THE MOVING PNEUMATIC WHEEL

Prediction of soil sinkage is based on modeling of interrelated wheel and soil deformations along the wheel-soil contact surface under different operating conditions. Several assumptions were made for this model: the soil serves as a plastic non-linear medium, the wheel moves in steady

[1] Graduate student, Faculty of Agricultural engineering, Technion – Israel Institute of Technology, Haifa, ISRAEL, agroset@techunix.technion.ac.il.

[2] Associate Professor, Faculty of Agricultural engineering, Technion – Israel Institute of Technology, Haifa, ISRAEL, agshmilo@techunix.technion.ac.il.

state condition at a low velocity and the wheel-soil interaction is two-dimensional (plane strain problem). Therefore, all the values are presented in regard to the width unit of the wheel.

According to the above assumptions the rut formation z_0 under the moving pneumatic wheel is caused by the vertical load, applied to the wheel and configuration of the wheel-soil contact surface. A well-known approach to this problem is the representation of the contact surface by means of a mathematical curve. The most widespread suggestions in literature for presenting this surface include a circular arc of an equivalent rigid wheel, combined with either the unloaded contour of the tire or with straight sections (Bekker, 1960; Fujimoto, 1977).

The current work assumes that the contact surface under the moving wheel can be represented in parabolic form in the longitudinal direction with the vertex in the rear point *0* of contact (Fig.1).

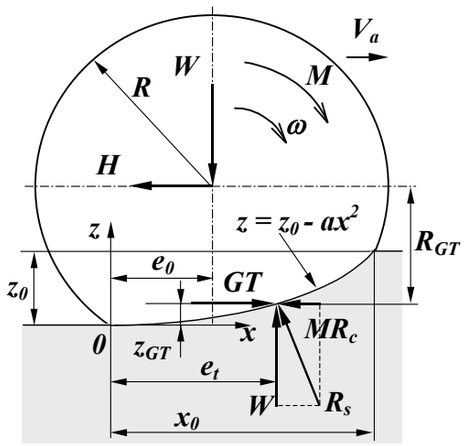

Fig. 1. Equilibrium of the moving driven wheel.

The contact surface can be represented by a parabolic curve equation:

$$z = z_0 - ax^2 \tag{1}$$

where: z_0 – rut depth, [m]; x – horizontal coordinate, [m]; and a – parameter of the parabolic equation, [m^{-1}].

In comparison with the 'circular' approaches, the 'parabolic' one allows for much simpler mathematical processing, which enables a closed form solution of the wheel-soil interaction. The divergence between the 'parabolic' and 'circular' approaches is smaller than the second order term when we expand them into a series.

Modeling of the Wheel-Soil Contact Surface

Modeling of the wheel-soil contact surface is based on the well-known approach originally suggested by Bekker (1960, 1962). The vertical soil pressure-sinkage relationship for a plate penetrating into homogeneous terrain is described as:

$$p_s = \left(\frac{k_c}{b} + k_\phi\right) z^n \tag{2}$$

where: p_s – vertical soil pressure, [kPa]; k_c – cohesive modulus of deformation, [$kN/m^{(n+1)}$]; k_ϕ – frictional modulus of deformation, [$kN/m^{(n+2)}$]; n – exponent of deformation; b – smaller dimension of the loading area (width of the wheel), [m]; and z – soil sinkage, [m].

The contact surface in the proposed parabolic form is found from equilibrium of the wheel in the vertical direction. The vertical load W on the moving wheel is equal to the resultant of the vertical ground pressure acting on the wheel-soil contact surface:

$$W = \int_0^{x_0} p_s b\,dx = b\left(\frac{k_c}{b} + k_\phi\right) \int_0^{x_0} z^n dx \tag{3}$$

where: W – vertical load, applied to the wheel, [kN]; b – width of the wheel, [m]; and dx - length of infinitesimal contact area, [m].

The values of k_c, k_ϕ and n are derived experimentally, according to the procedure described by Bekker (1960) and Wong (1993). Considering the expression (1), the force equilibrium (3) results in:

$$W = \frac{(k_c + bk_\phi)}{3}\sqrt{\frac{z_0}{a}}z_0^n(3-n) \tag{4}$$

The well-known solution for the rigid wheel of diameter D was derived by Bekker (1960, 1962):

$$W = \frac{(k_c + bk_\phi)}{3}\sqrt{z_0 D}z_0^n(3-n) \tag{5}$$

It is obvious that this 'circular' solution is the partial case of the proposed 'parabolic' model and can be derived from (4) after substituting the factor $\sqrt{1/a}$ by $\sqrt{D}$. Thus, the physical meaning of the parameter a of the parabola is the inverse value of the equivalent rigid wheel diameter.

Modeling of Tire Deflections

The loads acting on the driven moving wheel result in surface traction along the wheel-soil contact area. The vertical component of the surface traction is caused by the deflection of a moving pneumatic wheel, affected by the vertical load W. In order to adjust the parabolic form of the contact surface to the deflection of a moving pneumatic wheel, its state of equilibrium in the vertical direction is analyzed (Fig. 2).

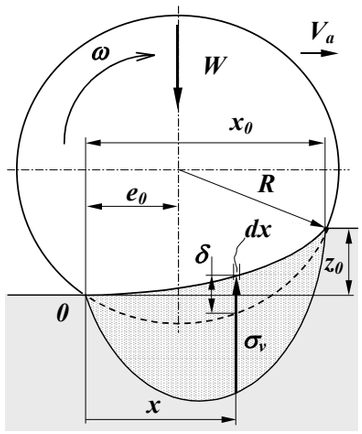

Fig. 2. Force equilibrium of a moving wheel in the vertical direction.

Deformations of the wheel are assumed to be linear elastic. Therefore, the elementary vertical load p_v and the vertical component of the surface traction σ_v acting on the contact area with width b and length dx can be found as follows:

$$p_v = k_v \delta\, dx \tag{6}$$

$$\sigma_v = \frac{p_v}{bdx} = \frac{k_v \delta}{b} \tag{7}$$

where: p_v – elementary vertical load, [kN]; σ_v – vertical component of the surface traction, [kPa]; k_v – coefficient of vertical stiffness of the wheel, [$kN/m/m$]; and δ – vertical displacement of the elementary contact area of the wheel, [m].

The vertical displacement δ of the elementary area of the parabolic contact surface is:

$$\delta = \sqrt{R^2 - (x - e_0)^2} - \sqrt{R^2 - e_0^2} + ax^2 \tag{8}$$

where: R – unloaded radius of the wheel, [m]; x – coordinate of the elementary contact area, [m]; and e_0 - eccentricity of the center of the wheel in relation to the rear point *0* of the contact surface, [m].

The distribution of the vertical component of the surface traction along the wheel-soil contact surface is shown in Fig. 2. The force equilibrium of a moving wheel in the vertical direction can be expressed as:

$$W = \int_x p_v = \int_0^{x_0} k_v \delta dx \tag{9}$$

where: W – vertical force acting on the wheel, [kN]; and x_0 – length of the contact surface, [m].

Expression (9) results in the following analytical solution:

$$W = k_v \left\{ \frac{a x_0^3}{3} - \sqrt{R^2 - e_0^2}\left(x_0 - \frac{e_0}{2}\right) + \frac{(x_0 - e_0)}{2}\sqrt{R^2 - (x_0 - e_0^2)} + \frac{R^2}{2}\left(arcsin\left(\frac{x_0 - e_0}{R}\right) + arcsin\left(\frac{e_0}{R}\right)\right)\right\} \tag{10}$$

The eccentricity e_0 of the center of the wheel is found geometrically according to Fig. 2 as:

$$e_0 = \frac{x_0}{2}\left(1 - a\left(\sqrt{\frac{4R^2}{1 + (a x_0)^2} - x_0^2}\right)\right) \tag{11}$$

The coefficient k_v of the examined wheel can be evaluated on the basis of the load-displacement relationship for certain values of inflation pressure P_{in} and vertical load W as follows:

$$k_v = \frac{W}{\left[R^2\, arcsin\left(\frac{x_0}{R}\right) - x_0(R - \Delta)\right]} \tag{12}$$

where: Δ – deflection of the wheel on hard surface [m].

Prediction of Rut Depth under a Moving Wheel

The parameter a of the parabolic contact surface and the rut depth z_0 under the moving wheel are derived from a simultaneous solution of equations (4) and (10). The proposed model was validated using two cases of wheel-soil interaction: rigid wheel and pneumatic wheel on soft soil. The relationships between rut depth and vertical load as well as between deformation and wheel stiffness are yielded by data from previous experiments presented in the literature. The predicted results were compared with the experimental data reported by Pope (1969), Shmulevich (1975), Gee-Clough (1976), Muro (1993) and Du Plessis (1993). The correlation between predicted and experimental data is shown in Fig. 3.

The proposed model shows reasonable accuracy in simulating rut depth, assuming a parabolic contact surface between the wheel and soil.

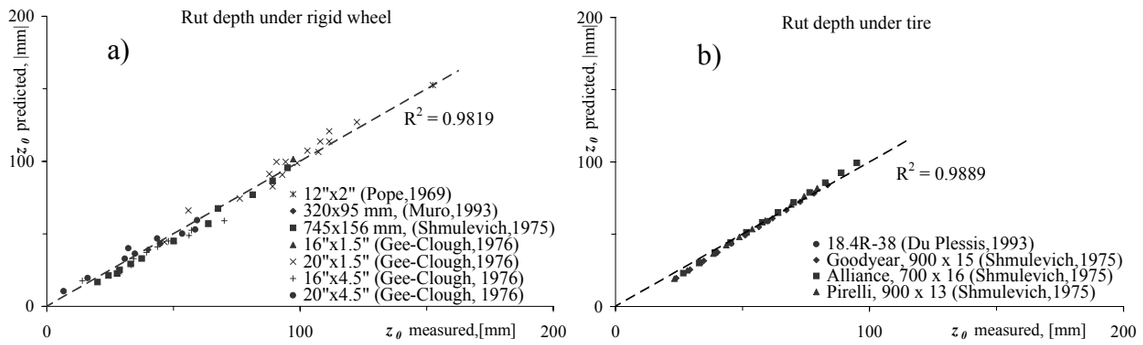

Fig. 3. Correlation between predicted and measured sinkage of the soil: a) under rigid wheel; b) under pneumatic wheel.

SOIL SHEAR DISPLACEMENTS AND SLIP OF THE MOVING WHEEL

The kinematic aspect of the wheel-soil interaction includes the analysis of relative displacements and velocities of wheel and soil, slip, etc. In order to calculate the relationship between tractive effort and slip of a moving wheel, the shear displacement development along the wheel-soil interface has to be determined first. The shear displacement developed along the contact area of the wheel may be derived from a similar analysis for a rigid wheel, described by Wong and Reece (1967).

The absolute velocity of any peripheral point *B* on the wheel can be found according to Fig. 4.

$$\overline{V} = \overline{V_a} + \overline{V_\omega} \tag{13}$$

where: $\overline{V}$ – absolute velocity of the peripheral point *B* on the wheel, [*m/s*]; $\overline{V_a}$ – actual longitudinal velocity of the wheel, [*m/s*]; and $\overline{V_\omega}$ – velocity of the point *B* in relation to the center of the wheel, [*m/s*].

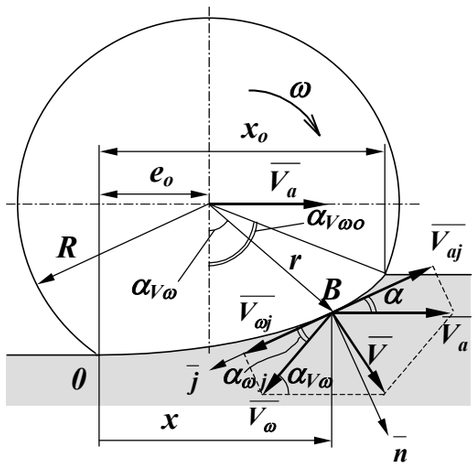

Fig. 4. Illustration of slip velocity.

The absolute velocity of point *B* can be resolved along the axes $\overline{n}$ and $\overline{j}$ into the normal and tangential components. The latter is slip velocity $\overline{V_j}$. The positive direction of the $\overline{j}$ axis corresponds to the positive direction of the moving wheel's angular velocity. Slip velocity can be derived as the vector sum of projections of absolute velocity components on the $\overline{j}$ axis. Based on expression (13) the following equation can be calculated:

$$\overline{V_j} = \overline{V_{aj}} + \overline{V_{\omega j}} \tag{14}$$

where: $\overline{V_j}$ – slip velocity of point *B*, [*m/s*]; $\overline{V_{aj}}$ – tangential projection of the actual longitudinal velocity of the wheel, [*m/s*]; and $\overline{V_{\omega j}}$ – tangential projection of velocity of the point *B* in relation to the center of wheel, [*m/s*].

The magnitude of slip velocity can be evaluated be rewriting equation (14):

$$V_j = V_{\omega j} - V_{aj} = \omega\, r \cos\alpha_{\omega j} - V_a \cos\alpha \tag{15}$$

where: ω – angular velocity of the wheel: $\omega = \frac{d(\alpha_{V\omega})}{dt}$, [$s^{-1}$]; *r* - radius vector of point *B* from wheel center, [*m*]; V_a – magnitude of the actual longitudinal velocity of the wheel, [*m/s*]; $\alpha_{\omega j}$ – angle between the velocity of the point *B* in relation to the center of the wheel and its projection on the $\overline{j}$ axis, [*rad*]; α – angle between *x*-axis and tangent at the point *B*, [*rad*]; and $\alpha_{V\omega}$ – angle between the vertical axis and position of the radius-vector to the current point on the wheel-soil interface, [*rad*].

The soil shear displacement at point B can be found by integrating the slip velocity over time:

$$j = \int_0^t V_j dt = -\int_{\alpha_{V\omega 0}}^{\alpha_{V\omega}} \left(\omega r \cos\alpha_{\omega j} - V_a \cos\alpha\right) \frac{d(\alpha_{V\omega})}{\omega} = \int_{\alpha_{V\omega}}^{\alpha_{V\omega 0}} \left(r\cos\alpha_{\omega j} - \frac{V_a}{\omega}\cos\alpha\right) d(\alpha_{V\omega}) \tag{16}$$

where: j – shear displacement of the soil at point B, [m].

Since the form of the contact surface is known, all geometrical relationships are found based on trigonometry and differential geometry as functions of x; and equation (16) can be rewritten as:

$$j = \int_x^{x_0} \frac{\left(ax(x-2e_0) + \sqrt{R^2 - e_0^2} - \frac{V_a}{\omega}\right)\left(ax(x-2e_0) + \sqrt{R^2 - e_0^2}\right)}{\sqrt{1+(2ax)^2}\left(\left(ax^2 - \sqrt{R^2 - e_0^2}\right)^2 + (x-e_0)^2\right)} dx \tag{17}$$

The analytical solution of this integral is complex, and therefore a numerical approach is needed.

The current solution can be applied in the driving mode of the moving wheel as well as in the braking mode. For instance, in full braking condition, expression (17) has a simple analytical solution. It can be simplified by assuming zero angular velocity. Thus, slip velocity (15) in this case is calculated according to:

$$V_j = -V_{aj} = -V_a \cos\alpha \tag{18}$$

Shear displacement of the soil along the contact surface is calculated as follows:

$$j = \int_0^t V_j dt = \int_0^x \left(-V_a \cos\alpha\right) \frac{dx}{V_a} = -\int_0^x \frac{dx}{\sqrt{1+(2ax)^2}} = -\frac{1}{2a} ln\left(2ax + \sqrt{1+(2ax)^2}\right) \tag{19}$$

It can be seen, that the modeled shear displacement in full braking condition has a negative value, which means that the shear displacement is in the opposite direction of the angular velocity.

MODELING OF THE GROSS TRACTION FORCE

The infinitesimal area ds of the wheel-soil contact surface (Fig. 5) is subjected to the surface traction and results in an elementary force, which can be presented by normal and tangential components σds and τds. On the other hand, the vertical and horizontal components of this force are found as follows:

$$\begin{cases} p_h = (\sigma ds)\sin\alpha - (\tau ds)\cos\alpha \\ p_v = (\sigma ds)\cos\alpha + (\tau ds)\sin\alpha \end{cases} \tag{20}$$

where: ds – infinitesimal contact area, [m^2]; p_h – horizontal component of the elementary force, acting on the contact area ds, [kN]; and σ, τ – normal and shear stresses acting on the contact area ds, [kPa].

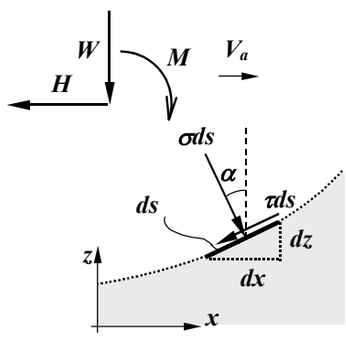

Fig. 5. Elementary forces applied to the soil contact area ds.

Considering

$$ds \sin\alpha = bdz \text{ and } ds \cos\alpha = bdx \tag{21}$$

the system of equations (20) can be rewritten as follows:

$$\begin{cases} \dfrac{p_h}{bdx} = \sigma \dfrac{dz}{dx} - \tau \\ \dfrac{p_v}{bdx} = \sigma + \tau \dfrac{dz}{dx} \end{cases} \tag{22}$$

The shear stress-displacement relationship along the wheel-soil contact surface is described by the model suggested by Janosi and Hanamoto, (1961):

$$\tau = (c + \sigma \tan\phi)(1 - e^{-j/K}) \tag{23}$$

where: K – shear deformation modulus, [m]; c – soil cohesion, [kPa]; and ϕ – angle of internal friction, [rad].

The value of shear deformation modulus K can be evaluated experimentally, according to the technique described by Wong (1993). Considering the relationships (23), (6), (7) the horizontal component of the surface traction p_h is derived from the system of equations (22) as follows:

$$p_h = \frac{\sigma_v \left(2ax - \tan\phi(1 - e^{-j/K})\right) - c\left(1 - e^{-j/K}\right)\left((2ax)^2 + 1\right)}{1 + 2ax(1 - e^{-j/K})\tan\phi} bdx \tag{24}$$

The resultant of the surface traction in the horizontal direction is equal to the gross traction force GT and can be evaluated by integrating p_h along the wheel-soil contact area:

$$GT = \int_0^{x_0} p_h = \int_0^{x_0} \frac{\sigma_v \left(2ax - \tan\phi(1 - e^{-j/K})\right) - c\left(1 - e^{-j/K}\right)\left((2ax)^2 + 1\right)}{1 + 2ax(1 - e^{-j/K})\tan\phi} bdx \tag{25}$$

where GT – gross traction force, [kN].

MOTION RESISTANCE OF THE WHEEL

Motion resistance is caused by soil reaction, bulldozing resistance and various internal losses. In order to evaluate the motion resistance, one should analyze each component and summarize them. The bulldozing resistance and the internal losses can be evaluated on the basis of well-known approaches (Wong, 1993). Since most of the resistance is due to soil reaction (Bekker, 1960), only this component is analyzed in this paper.

The soil reaction R_s is the resultant of surface traction along the contact surface (Fig. 1). It can be resolved into vertical and horizontal components. The vertical component equals to the vertical load W acting on the wheel and has a forward eccentricity relative to the wheel center. The eccentricity of the soil reaction relative to the rear point of contact can be calculated from the equilibrium of the moving wheel:

$$e_t = \frac{k_v}{W}\left[\frac{z_0^2}{4a} + \frac{\sqrt{R^2 - (x_0 - e_0)^2}}{3}\left((x_0 - e_0)\left(x_0 + \frac{e_0}{2}\right) - R^2\right) + \right.$$
$$\left. + \frac{\sqrt{R^2 - e_0^2}}{3}\left(R^2 + \frac{e_0^2}{2} - \frac{3}{2}x_0^2\right) + \frac{R^2 e_0}{2}\left(\arcsin\left(\frac{x_0 - e_0}{R}\right) + \arcsin\left(\frac{e_0}{R}\right)\right)\right] \tag{26}$$

where: e_t – eccentricity of the soil reaction relative to the rear point of contact, [m].

Both the vertical load applied on the axle and vertical soil reaction produce a couple of forces, resulting in the moment M_r, in opposite direction to the driving torque M applied to the wheel:

$$M_r = W_t\,(e_t - e_0) \tag{27}$$

where: M_r – moment due to eccentricity of the vertical soil reaction, [$kN{\cdot}m$].

The horizontal component of the soil reaction is the motion resistance force of the wheel due to soil compaction MR_c. The compaction motion resistance is calculated from the energy balance of soil deformation under a moving wheel. The compaction resistance is a function of soil properties, wheel width b and rut depth z_0 (Fig. 1).

The compaction resistance is derived in the same way as for a rigid wheel (Bekker, 1960). Applying this expression is justified by its non-dependence on the form of the contact surface:

$$MR_c = \frac{(k_c + bk_\phi)}{(n+1)} z_0^{(n+1)} \tag{28}$$

where: MR_c – compaction resistance of the moving wheel, [kN].

TRACTION PERFORMANCE SIMULATION OF A WHEEL

The point where the gross traction force is applied (Fig. 1) can be found after equilibrium analysis of the moments, applied on infinitesimal elements of the wheel-soil contact surface:

$$z_{GT} = \frac{1}{GT}\int_0^{x_0} p_h z = \frac{ab}{GT}\int_0^{x_0} \frac{\sigma_v\left(2ax - \tan\phi(1-e^{-j/K})\right) - c\left(1-e^{-j/K}\right)\left((2ax)^2+1\right)}{1+2ax(1-e^{-j/K})\tan\phi} x^2 dx \tag{29}$$

where: z, z_{GT} – vertical distances of the elementary force p_h and the gross traction force, from the bottom of the rut respectively, [m].

The distance from the center of the wheel to the point where the gross traction force is yielded, can be calculated from the geometry in Fig. 1 as follows:

$$R_{GT} = \sqrt{R^2 - e_0^2} - z_{GT} \tag{30}$$

where: R_{GT} – distance from the center of wheel to the gross traction force, [m].

The driving torque that should be applied to the wheel in order to reach the required value of gross traction force can be calculated as:

$$M_{GT} = GT{\cdot}R_{GT} \tag{31}$$

where: M_{GT} – driving torque, required by gross traction, [$kN{\cdot}m$].

The total driving moment M should support the moment caused by the gross traction force M_{GT} and the moment M_r:

$$M = M_{GT} + M_r \tag{32}$$

The net traction force is calculated as:

$$H = GT - MR_c \tag{33}$$

In order to predict the traction performance of a moving wheel, the mathematical expressions derived above were used. A special procedure was developed, using Matlab software, to calculate wheel performance as a function of soil and wheel properties versus wheel slip. For given operating conditions, a stationary vertical equilibrium results in a predictable parabolic contact surface between wheel and soil. Based on this predicted surface, shear soil displacement and related stresses are calculated for various slip values, resulting in a prediction of gross traction, wheel torque and motion resistance.

The modeled traction performance was verified by experimental data reported for the rigid wheel (Muro, 1993) and tire (Thangavadivelu, 1994) operating in the driving mode. Carcass stiffness K_c and inflation pressure dependence ΔK_p of the 9.5-16R-1 tire are equal to the values, reported by Lines and Murphy (1991), for an inflation pressure of *1.5 bar*. The operating conditions, used

for the simulations, are cited according to the above-mentioned sources and are presented in Table 1.

Table 1. Soil properties and wheel specifications used for the simulations.

Wheel specifications						Soil properties					
Wheel	W	ΔK_p	K_c	b	D	k_c	k_ϕ	n	c	ϕ	K
	kN	*kN/m/bar*	*kN/m*	*mm*	*Mm*	$N/cm^{(n+1)}$	$N/cm^{(n+2)}$	-	*kPa*	*deg*	*mm*
Rigid wheel	1.52	–	–	95	320	48.1	36.47	0.757	0.0	22.9	6.0
Tire 9.5-16R-1	4.00	134	86	240	850	2.1	4.70	1.400	6.3	18.3	8.0

The predicted net traction force and the experimental data are shown versus slip in Fig. 6. The suggested method shows reasonable agreement between modeled and reported results: for the tire and for the rigid wheel R^2 is equal to *0.9687* and *0.8656* respectively.

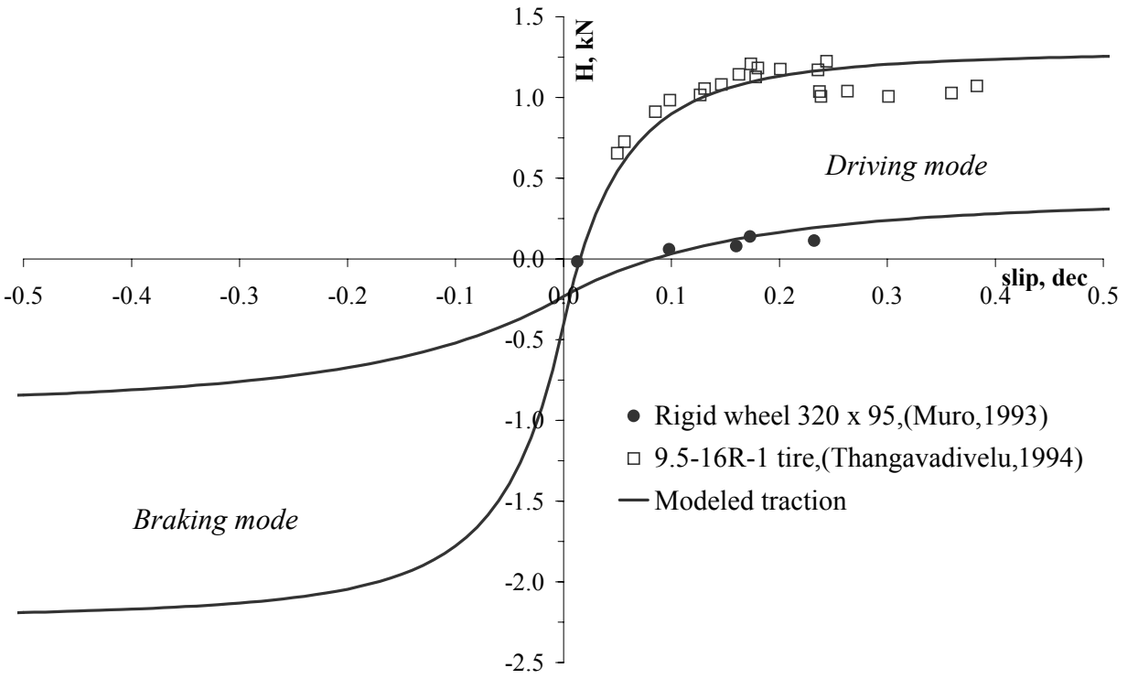

Fig. 6. Comparison between predicted and measured net traction force of a driven wheel.

The suggested method is applied for prediction of traction performance for a single wheel in both driving and braking modes. Traction performance of a driven wheel operating in these modes is not symmetrical under the same conditions. The force required to pull the wheel in braking mode is greater than the traction force that is developed by the wheel in driving mode.

Under the specified operating conditions, the net traction force achieved by the tire (Table 1) is about *1.25 kN* in the driving mode (similar to the measured value). However, to pull a full braking tire requires a force of about *2.2 kN*, which is *75%* more than the force achieved in the driving mode. The net traction force developed by the rigid wheel in driving mode is not larger than *0.3 kN*. On the other hand, the predicted value of the traction force required for pulling the wheel in braking mode can reach a maximum value of close to *0.85 kN*, which is about three times higher.

CONCLUSIONS

1. The semi-empirical model for prediction of the traction performance of a driven wheel was developed, assuming the wheel-soil contact surface is parabolic.

2. The proposed method was successfully verified by the experimental data reported in literature.

3. Traction performance of a driven wheel can be predicted both for driving and braking modes.

4. The proposed model demonstrates significant non-symmetry of the traction wheel performance for driving and braking modes. The braking force developed in the braking mode is significantly greater than the traction force reached by the wheel in driving mode.

5. This method can serve as a comprehensive tool for predicting off-road vehicle performance.

REFERENCES

Bekker, M.G. 1960. *Off-the-road locomotion*. Ann Arbor: The University of Michigan Press.

Bekker, M.G. 1962. *Theory of land locomotion*. Ann Arbor: The University of Michigan Press.

Du Plessis, H.L.M. and G.Venter. 1993. Soft surface lateral forces and force modeling for a tractor tyre. *Journal of Terramechanics.* Vol. 30(2), p.101-110.

Fujimoto,Y. 1977. Performance of elastic wheels on yielding cohesive soils. *Journal of Terramechanics*. Vol. 14(4), p. 191 - 210.

Gee-Clough, D. 1976. The Bekker theory of rolling resistance amended to take account of skid and deep sinkage. *Journal of Terramechanics*. Vol. 13(2), p. 87-105.

Janosi, Z. and B.Hanamoto. 1961. The analytical determination of drawbar pull as a function of slip for tracked vehicles in deformable soils. In *Proceedings of the 1st International Conference on the Mechanics of Soil-Vehicle Systems*. June 12-16. Torino, Italy.

Lines, J.A. and K. Murphy. 1991. The stiffness of agricultural tractor tyres. *Journal of Terramechanics*. Vol. 28 (1), pp. 49-64.

Muro,T. 1993. Tractive performance of a driven rigid wheel on soft ground based on the analysis of soil-wheel interaction. *Journal of Terramechanics*. Vol. 30(5), p. 351-369.

Pope, R.G. 1969. The effect of sinkage rate on pressure sinkage relationships and rolling resistance in real and artificial clays. *Journal of Terramechanics*. Vol. 6(4), p. 31-38.

Shmulevich, I., D.Wolf and I.Leviticus. 1975. Laboratory criteria for selecting alternative vehicle tires. Technion – Israel Institute of Technology. Haifa. Publication # 249.

Thangavadivelu, S., R.Taylor, S Clark and J. Slocombe. 1994. Measuring soil properties to predict tractive performance of an agricultural drive tire. *Journal of Terramechanics*. Vol. 31(4), pp. 215-225.

Wong, J.Y. and A.R.Reece. 1967. Prediction of rigid wheel performance based on the analysis of soil wheel stresses. Parts I-II. *Journal of Terramechanics*. Vol. 4(1,2), p.p. 81 - 98, 7 - 25.

Wong, J.Y. 1993. *Theory of ground vehicles*. John Wiley & Sons Inc. New York.